Wireless Sensing of Epileptiform Activity

Senior Project

By
Wade Barnes

Electrical Engineering Department
California Polytechnic State University
San Luis Obispo
2010

TABLE OF CONTENTS

Section

Page

LIST OF TABLES AND FIGURES

Tables

Page

Figures

Acknowledgements

I would like to thank Dr. Prodanov for all of his help and advice throughout the course of this project. I would also like to thank Dr. Sungar for all of her help with the Matlab coding.

I. INTRODUCTION

Many natural phenomena exhibit characteristics of coupled chaotic oscillators, and recent research in this area shows promise for a wide array of engineering applications. One such system with this behavior is neuronal populations. The chaotic characteristics of individual neurons is known as spike-burst behavior, and many activities in the brain are thought to occur from the coupling of these individual neurons, creating a collective spike-burst pattern across an entire population of neurons. This phenomenon, collectively known as synchrony, appears in electrocorticographical (ECoG) recordings for several medical conditions including: Parkinson's disease, schizophrenia, and some types of epileptic seizures [1]. Since serious medical conditions exhibit these synchronous characteristics, being able to sense and record this behavior is a very exciting and important engineering application of this phenomenon.

II. BACKGROUND

The goal of this project is to show the signal characteristics of epileptiform activity through simulation, discuss modern medical advancements that sense this activity, and design a circuit that will wirelessly transmit this signal data and simultaneously supply power to the sensor. Matlab will be used to simulate individual neurons using the Hindmarsh-Rose (HR) neuron model, and to identify the regions of chaotic spike-burst behavior similar to the analysis seen in [1]. This spike-burst behavior will be applied to a coupled neuronal population in order to investigate the nature of epileptiform activity, which is an ensemble of coupled neural signals seen just prior to an epileptic seizure. This will be followed by a brief discussion of modern medical devices that are used to sense and eliminate epileptiform activity. Finally, a circuit will be designed and tested that will supply power to one of these modern sensors and also transmit the signal data back to the processor core for ECoG analysis of epileptiform activity.

III. REQUIREMENTS

The end goal of this project is to design and test a circuit that will wirelessly harvest power for circuit operation and transmit sensor data back to the power source for signal readout of epileptiform activity. In order to do this, three main objectives must be met:

1. Identify signal patterns associated with epileptiform activity using Matlab
2. Introduce medical devices currently being used in sensing epileptiform activity
3. Replace the wired connection through patient's skull that is currently used in these devices with a wireless power/data link

IV. MATLAB SIMULATIONS

In order to successfully sense epileptiform activity, it is essential to examine the signal characteristics of neuronal populations. This will be done through simulation using Matlab. This is a dimensionless analysis of neuronal interactions. However, the relative magnitudes of the variables in the following equations correctly approximate the signal characteristics of epileptiform activity, and dimensions will be applied later in the project. Individual neuronal behavior is approximated by the HR neuron model, which is governed by the following recursive equations:

$$\dot{x} = y - x^3 + 3x^2 - z + I_{ext} \quad (1)$$

$$\dot{y} = 1 - 5x^2 - y \quad (2)$$

$$\dot{z} = 0.006 * [4(x + 1.6) - z] \quad (3)$$

Matlab is used to solve this system with a fourth-order Runge-Kutta approximation method. In these equations, x is the neuron's membrane potential, y is associated with the fast current (Na^+ or K^+), z with the slow current (such as Ca^{2+}) [1], and the dots above each of these variables imply the next successive iteration in the recursive formulas. In the case of epilepsy, I_{ext} is a variable proportional to an externally applied direct current (DC), and will be used as the varying bifurcation parameter to induce spike-burst behavior (Appendix D). For signal analysis purposes, the main variable of interest is the membrane potential, x.

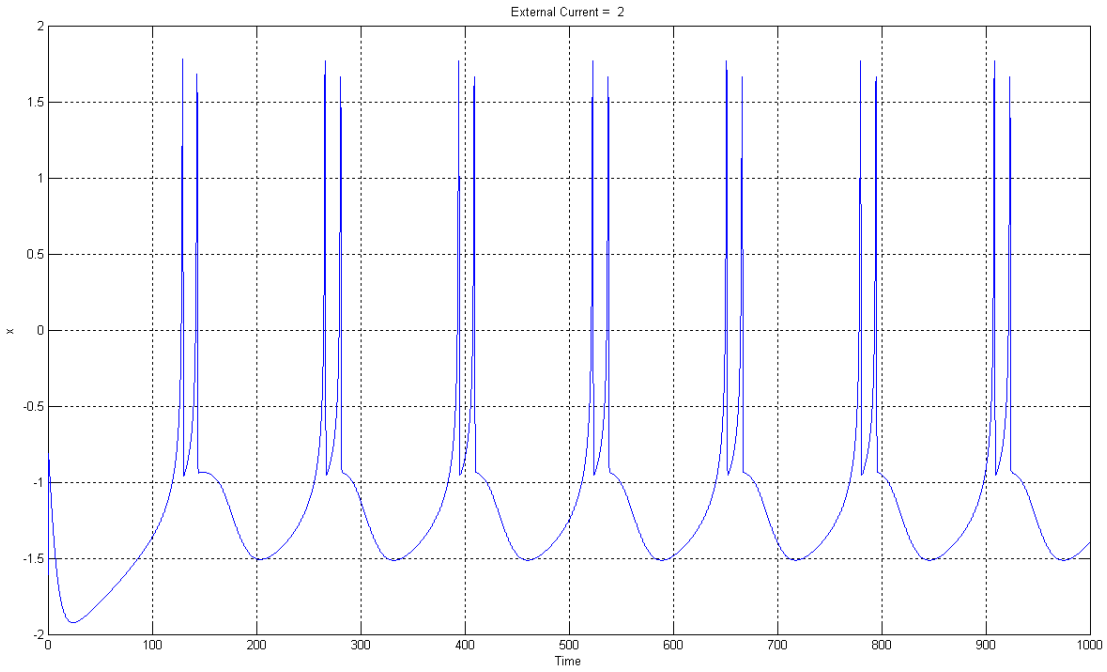

Fig. 1: Membrane Potential vs. Time with an External "Current" of 2 units

Figure 1 shows the same double spiked signal about every 200 increments of time, so it is periodic when the externally applied "current" is 2 units. Varying I_{ext} changes the periodicity of the membrane potential, and for particular values of I_{ext}, the membrane potential becomes chaotic. In Figure 2, a current of 3.2 units puts the membrane potential into a chaotic state.

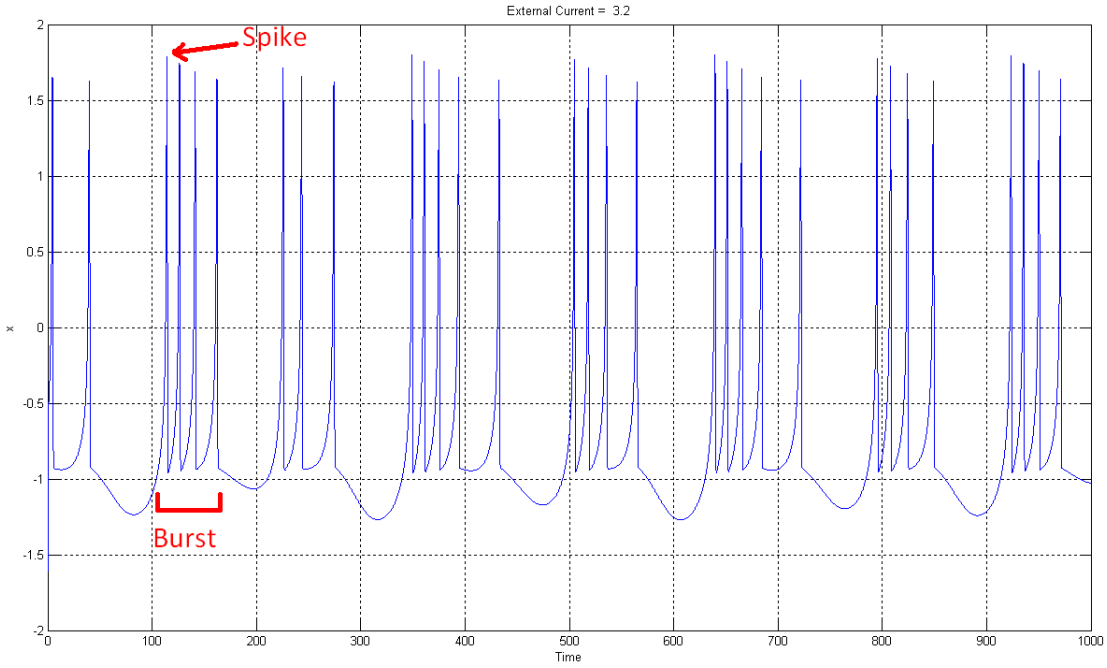

Fig. 2: Membrane Potential vs. Time with an External "Current" of 3.2 units

Figure 2 shows that, with an external "current" of 3.2 units, the distance between each consecutive spike is different. This aperiodic structure arises, because the system is now in a chaotic operating region. This chaotic operating region induces time-domain membrane potential characteristics known as spike-burst behavior, where an initial spike is followed by a burst packet as noted in Figure 2. In nonlinear systems analysis, it is convenient to graphically identify different operating regions with a bifurcation map.

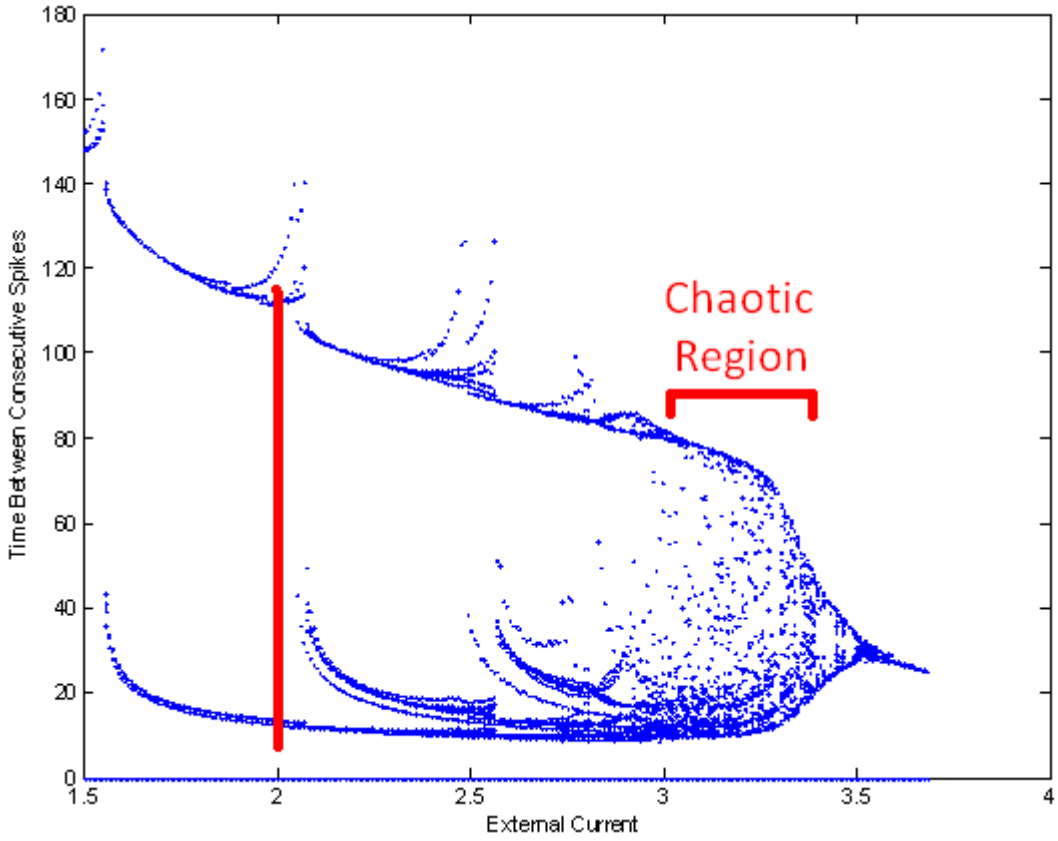

Fig. 3: Bifurcation Map of Time Between Membrane Potential Spikes vs. Varying I_{ext}

Using Figure 3, it is easy to analyze which values of I_{ext} will induce spike-burst behavior. By drawing a vertical line through the bifurcation map, the time between consecutive spikes of the membrane potential can be determined. As seen in Figure 3, drawing a vertical line at I_{ext}=2 units results in two distinct crossings. This means that there are two discrete times between membrane potential spikes for I_{ext}=2 units. This means that there is a periodic structure to the membrane potential

for all external current values that result in a discrete amount of crossings, and this is clearly shown in Figure 1 where I_{ext}=2 units. However, this structure breaks down in Figure 3 when I_{ext} is in the range from about 3 units to 3.4 units. This is known as the chaotic region. I_{ext}=3.2 units lies in the middle of this region, and results in the time-domain spike-burst behavior seen in Figure 2.

However, when taking an ECoG, the data is not collected from a single neuron. The data is taken from a population of neurons. Therefore a simulation must be done on a population of coupled chaotic oscillators, or, in this case, a population of coupled neurons exhibiting spike-burst behavior. Each neuron is coupled together with the neurons just before and after itself. This coupling is only done for the x term and changes Equation (1) to:

$$\dot{x}_n = y_n - x_n^3 + 3x_n^3 - z_n + I_{ext} + \varepsilon(x_{n-1} - 2x_n + x_{n+1}) \qquad (4)$$

where epsilon represents the coupling strength between the neurons, and the subscripted variables represent the neuron's relative position in the coupled chain of neurons. For example, if the neuron currently being analyzed is neuron #2, then it is coupled to neuron #1 (x_{n-1}) and neuron #3 (x_{n+1}). The code corresponding the differential equation solver and new system of equations can be found in

Appendices G and E, respectively. Figures 4 and 5 depict the effects of changing the coupling strength between the neurons.

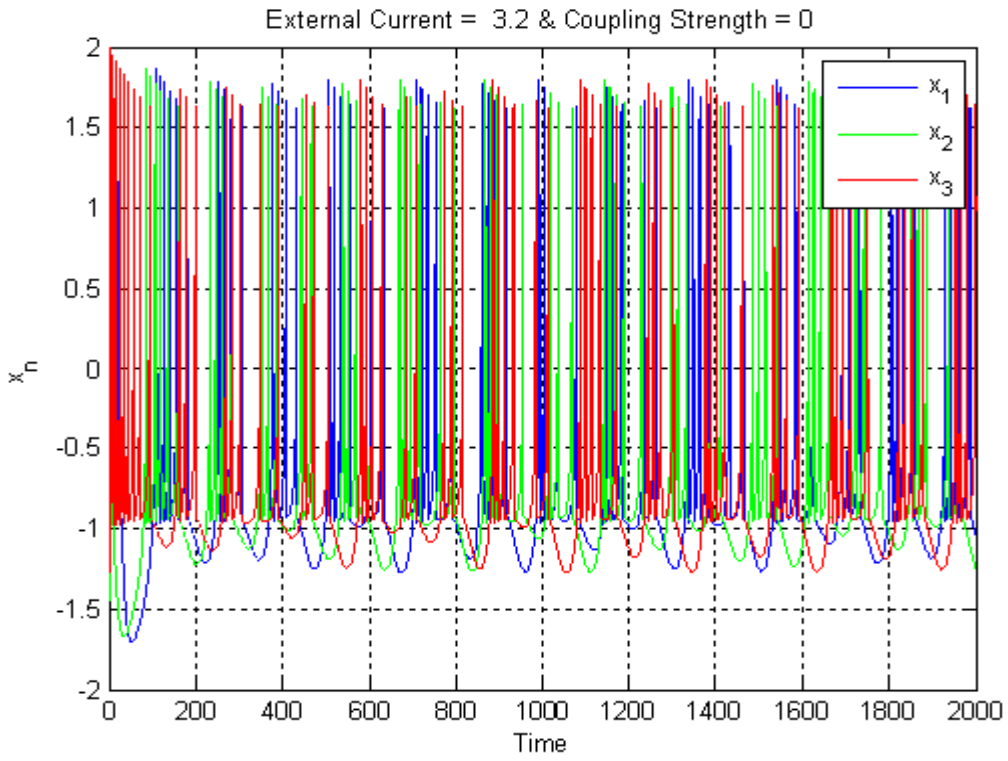

Fig. 4: Membrane Potential of Individual Spike-Burst Neurons with No Coupling

Figure 4 shows the membrane potential of 3 neurons each individually exhibiting spike-burst behavior, but with no coupling. While each individual neuron exhibits spike-burst behavior in this situation, an ECoG sees the entire population. In this case, the entire population does not exhibit a synchronous spike-burst effect, and this is a normal brain recording.

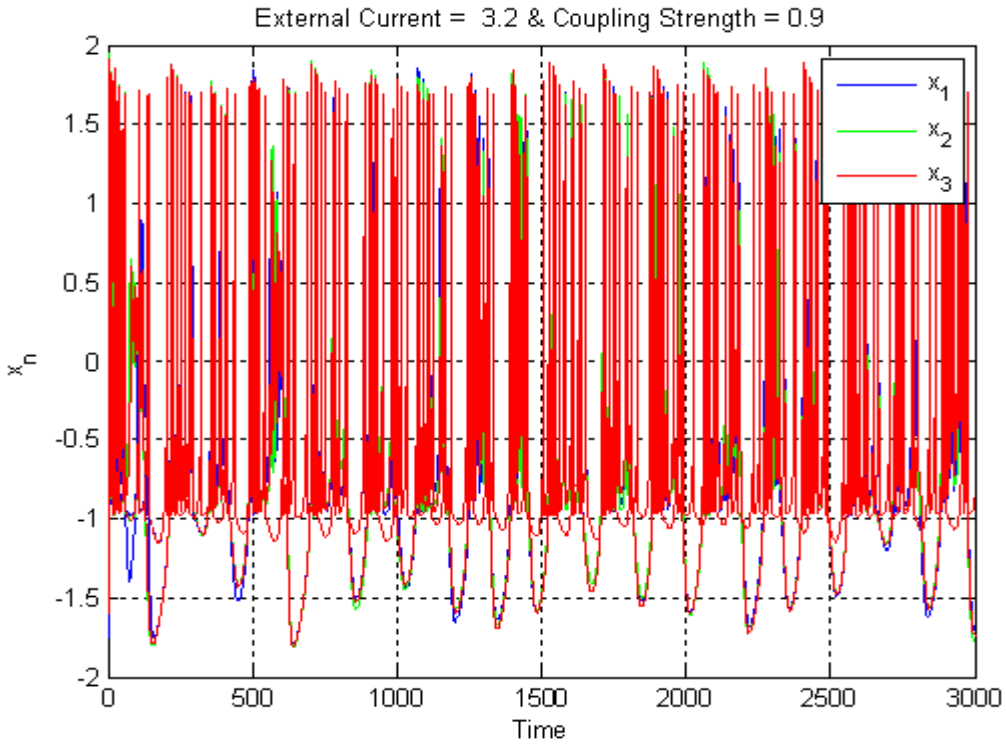

Fig. 5: Membrane Potential of Individual Spike-Burst Neurons with Strong Coupling

Figure 5 shows the membrane potential of 3 neurons each individually exhibiting spike-burst behavior, and the population has a strong coupling factor of ε=0.9. This strong coupling factor causes the individually chaotic neurons to synchronize into a spike-burst pattern across the entire population. While it is not entirely known whether epileptiform activity occurs from synchronization, as in Figure 5, or desynchronization of spike-burst activity, as in Figure 4, being able to identify synchrony is an extremely important measurement in the detection of

epileptic seizures [2]. The signal characteristics of epileptiform activity can be seen through these dimensionless simulations. Being able to discern between the chaotic synchronization and desynchronization of neuronal populations is the overall goal in the detection of epileptiform activity.

V. DESIGN

5.1 Overview

Several companies have recently made advancements in the detection and elimination of this epileptiform activity through external responsive neurostimulation devices. Since a majority of brain activity is made up of low frequency content, “the sampling frequency was set to 500 Hz” [3] for ECoG data. This is a relatively low sampling frequency when compared to modern consumer electronics, but it is sufficient for ECoG recordings. These devices contain three major components: sensor network placed at the patient’s seizure focus, battery/DSP core, and the neural stimulator for seizure prevention. Figure 6 shows a picture of a typical implantation of one such device.

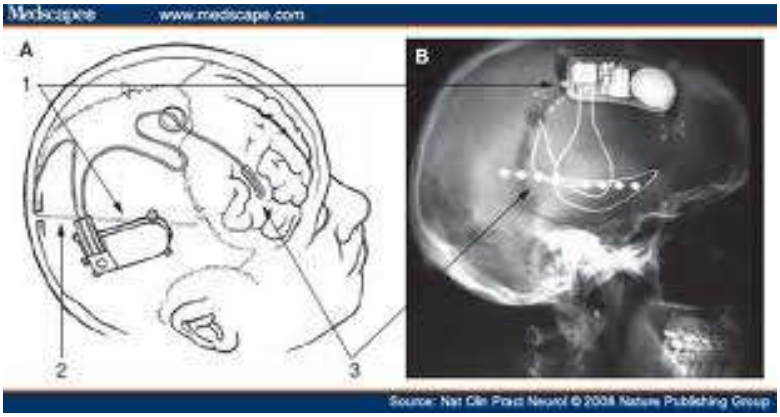

Fig. 6: Arrangement of Typical Responsive Neurostimulation Device [4]

Figure 6 shows that the battery/DSP core are implanted on the side of the head and are wired directly to the front of the brain at the location of the sensor network. This leaves the patient with a permanent hole in the skull. Using near-field coupling, this wired connection could be replaced with the network shown in Figure 7.

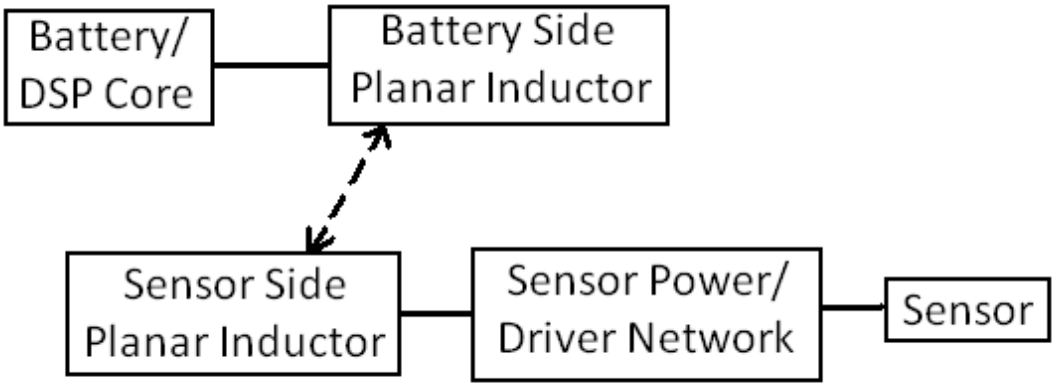

Fig. 7: Block Diagram of Wireless Power/Sensing Network

From Figure 7, the sensor will have a digital output. Since the relevant signal information is made up low frequency content, fairly accurate readings of the signal can be achieved by increasing the number bits in the digital output without requiring a large increase in the frequency of the digital output. The sensor network will be powered by the battery/DSP core through near-field inductive coupling. From this point forward, transmissions from the battery side planar inductor to the sensor side

planar inductor will be known as the downlink, and transmissions from the sensor side planar inductor to the battery side planar inductor uplink.

5.2 Planar Inductors

Since the device is to be implanted in the skull, size is a major issue. A planar inductor structure for near-field coupling is more suitable than a coiled structure, since it can be implanted flat against the skull. Radio frequency identification (RFID) tags are well suited for near-field coupling and are easy to manufacture. RFID tags have three standard operating frequency ranges: low frequency (LF), high frequency (HF), and ultra high frequency (UHF). It is ideal to use a higher frequency transmission for the downlink in order to minimize the size of the tags. However, it is not feasible to design a UHF tag in the current facilities, so a HF tag structure will be used for a proof of concept. RFSim99 © has a built-in planar inductor design tool. Using this, the square spiral inductance is calculated to be 3.1 uH.

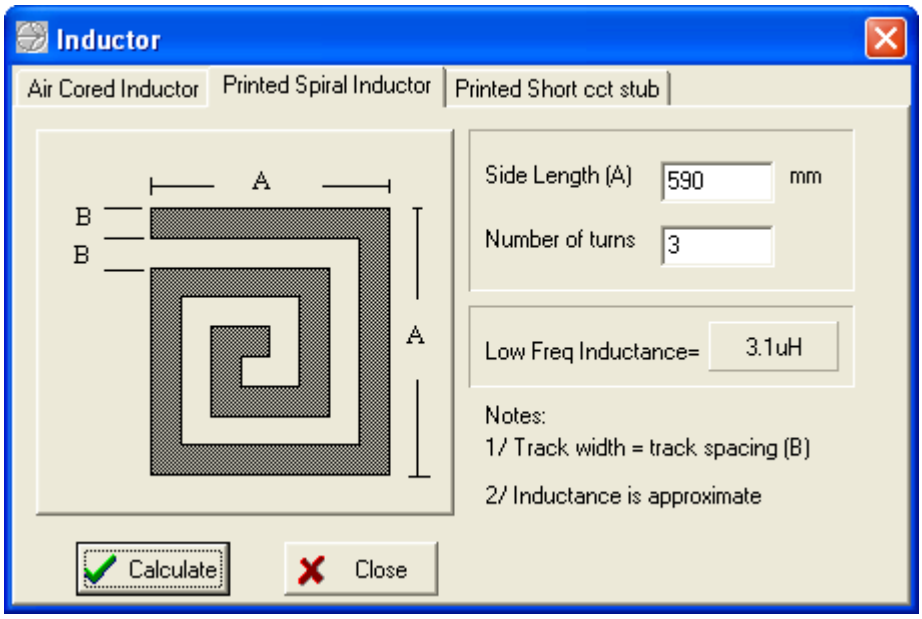

Fig. 8: Screenshot of Inductor Design

It is important to measure the actual inductance at this point in the project in order to carry out circuit simulations for the rest of the project. Using copper tape, a rectangular spiral inductor structure with an outer length of 590 mm is built. Due to slight variations from the simulation, the inductor is measured to be 1.0 uH. Placing the two similar inductor structures in close proximity to one another provides the near-field inductive coupling.

5.3 Theory of Operation

Using the near-field coupling of the inductors, a constant frequency can be transmitted via the battery side inductor to the sensor side inductor. This signal can be both positively and negatively rectified by inserting two diodes with opposing polarity in parallel on the sensor side inductor. Adding a capacitor in series with each of the diodes provides two DC voltage rails with opposing polarity. These rails can be used to power the sensor network.

The digital output of the sensor must now be sent via the uplink to the battery side inductor, L_1. This can be done by varying the effective load presented to the battery- a new effective battery side inductance, which will be called L_{1eff}. In order to vary the load presented to the battery side inductor, the load presented to the sensor side inductor, L_2, must vary. Since the sensor outputs digital data, the varying load requires only two distinct states. Therefore, the load presented to L_2 will be approximately open and short. L_{1eff} is given by the following relations:

$$open\ load: \qquad L_{1eff} = L_1 \qquad (5)$$

$$short\ load: \quad L_{1eff} = L_1(1 - k^2) \qquad (6)$$

where k is the coupling strength between the two inductors. This varying battery side inductor value changes the voltage presented to the battery side inductor, making the digital sensor data measurable on the battery side. Figure 9 shows a

schematic representing this theory of operation with an assumed coupling factor of 0.8, and Figure 10 shows the digital signal readout on the battery side with no capacitances included.

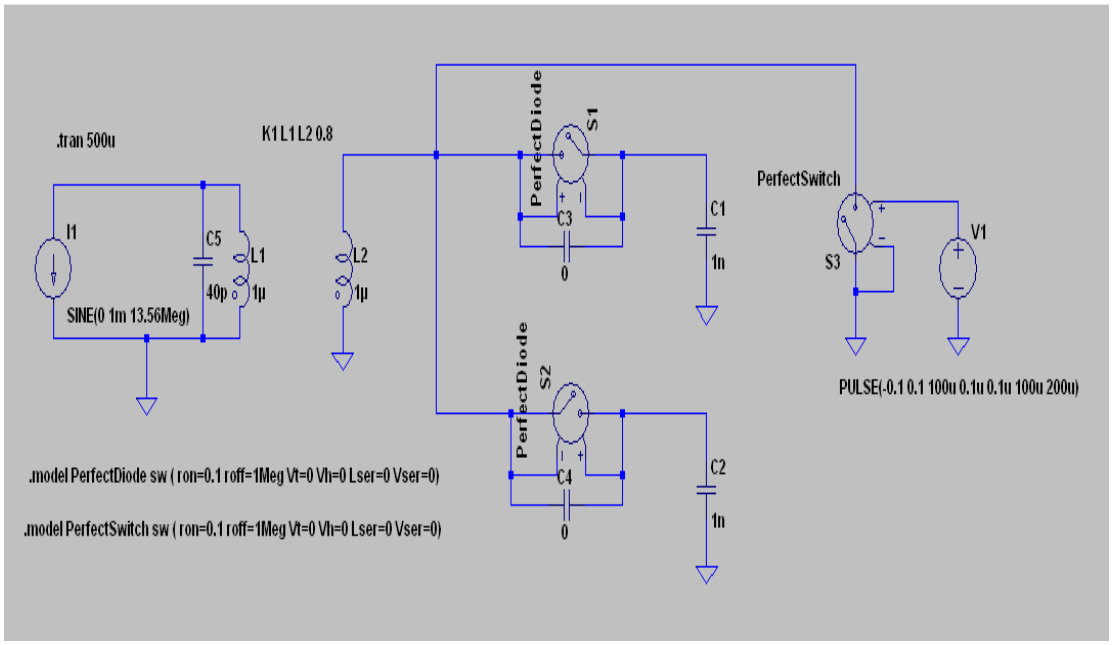

Fig. 9: Schematic of Ideal Operation in LTSPICE

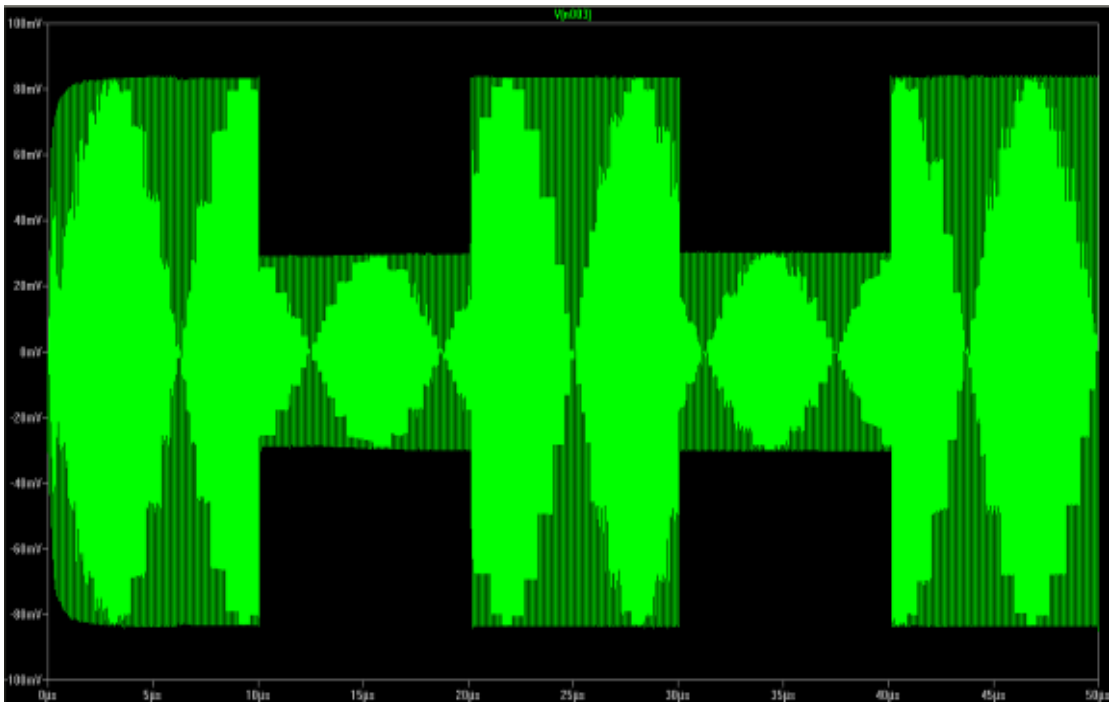

Fig. 10: Ideal Digital Sensor Simulation on Battery Side with No Capacitance in LTSPICE

Figure 10 is the simulated result of ideal diodes and switching discussed above, and represented in the schematic in Figure 9 with C5=0F. This has a 50 kHz data rate from the digital sensor output. Changing the value of C5 allows for tuning of the near-field coupling. Changing the value of C5 to 40 pF and the sensor data rate to 5 kHz changes the voltage across L1 and is shown in Figure 11.

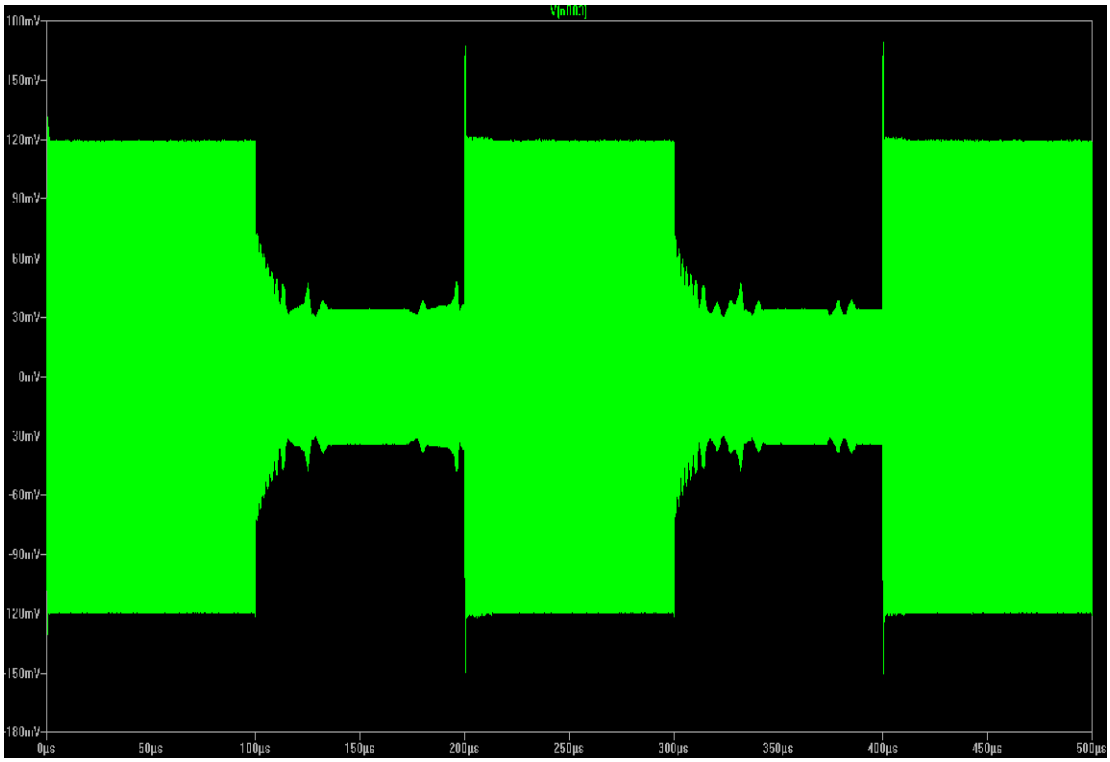

Fig. 11: Ideal Digital Sensor Simulation on Battery Side with C5=40pF in LTSPICE

Comparing Figures 10 and 11 presents an interesting tradeoff. The maximum peak-to-peak voltage is 150% larger in Figure 11 than it is in Figure 10. However, the increased capacitance causes a much slower roll-off of the signal shown in Figure 11. In order to maintain an accurate measurement, the sensor data rate had to be reduced from 50 kHz in Figure 10 to 5 kHz in Figure 11. For the actual design, no tuning capacitor will be included in order to maximize the sensor data rate.

5.4 Circuit Design

In order for the circuit to operate correctly, L_2 must have a load that can quickly act as a short or open. A MOSFET presents itself as a perfect candidate by operating it in saturation and cut-off modes. By connecting the MOSFET's drain and source in parallel with L_2, an effective short and open load situation is created by varying the gate voltage of the MOSFET to put it into saturation and cut-off modes. In order to ensure that the MOSFET goes fully into these operating modes, it is important that the gate voltage swings to sufficient voltages. This can be done by connecting a CMOS inverter between the sensor output and the gate voltage of the MOSFET. A schematic representing this description is shown in Figure 12.

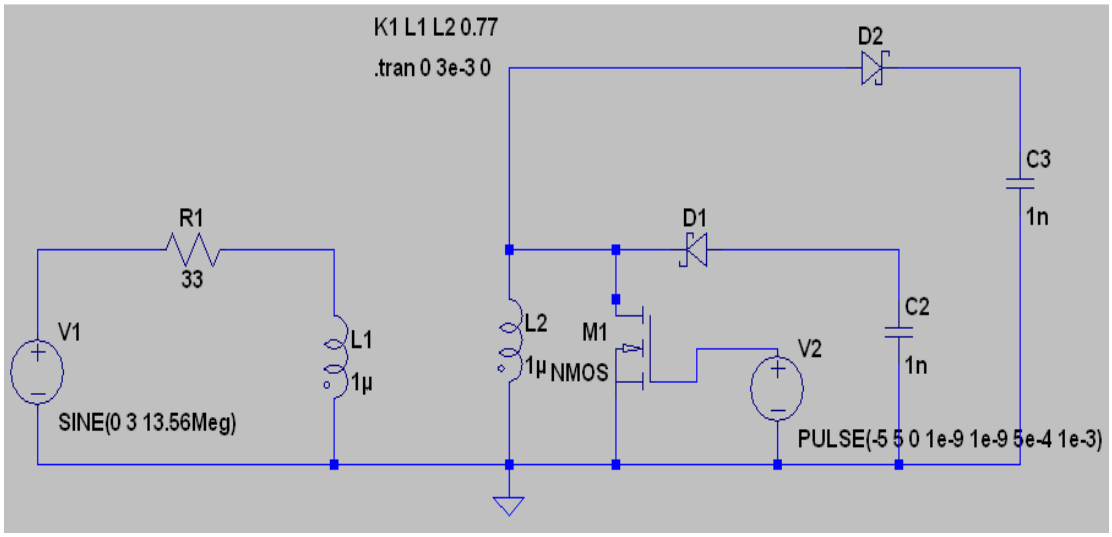

Fig. 12: Circuit Level Schematic Simulated in LTSPICE

The circuit shown in Figure 12 has a data rate of 1 kHz, and the voltage seen at the node connecting R1 and L1 appears in Figure 13.

Fig. 13: Voltage Seen at R1/L1 Node Corresponding to Digital Sensor Output

After simulating, a physical circuit was constructed and tuned, and the corresponding final circuit schematic is given in Figure 14.

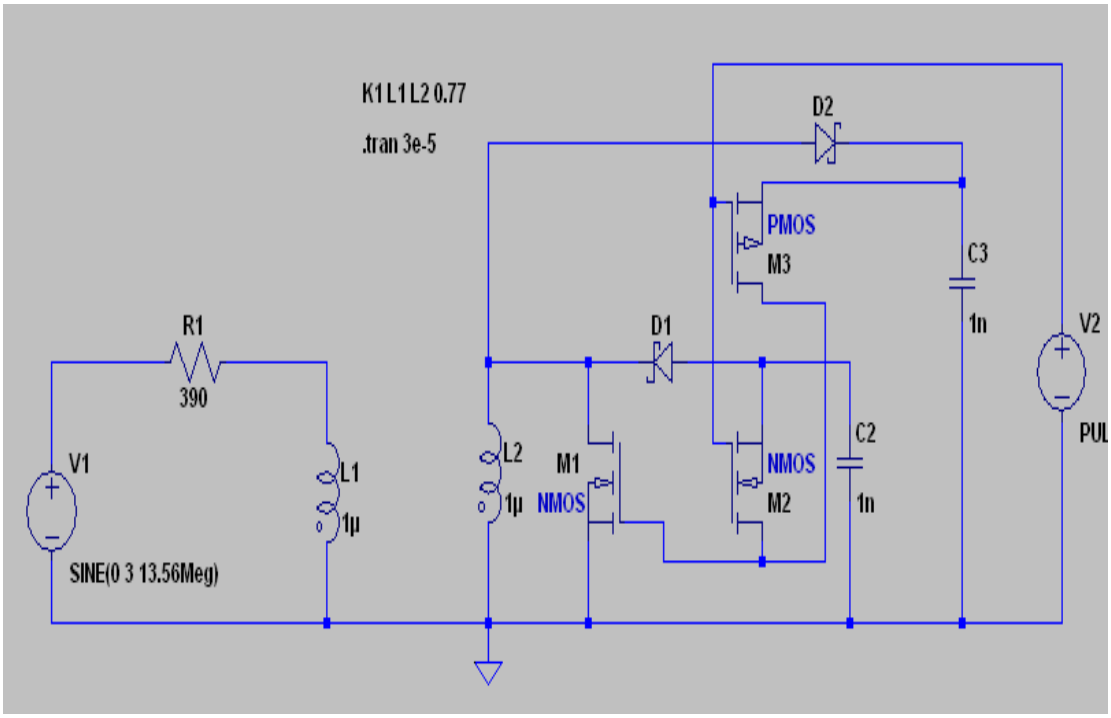

Fig. 14: Final Circuit Schematic

Figure 14 shows the final circuit schematic. L1 and L2 are the planar inductors discussed earlier. V1 is transmitted from the battery/DSP core area, and V2 is the digital sensor output. M2 and M3 make up the CMOS inverter. They get their power from the voltage rails created by D2/C3 and D1/C2. Finally, M1 is the MOSFET that creates the varying load.

VI. TESTING

Different portions of the circuit were tested individually prior to combining the different portions for the final test. First, the inductive coupling between the two planar inductors was tested by separating them by 5 mm, connecting a function generator to one of the inductors, and measuring the voltage on the other inductor with an oscilloscope. The coupling factor came out to approximately 0.77, and can be seen in Figure 15.

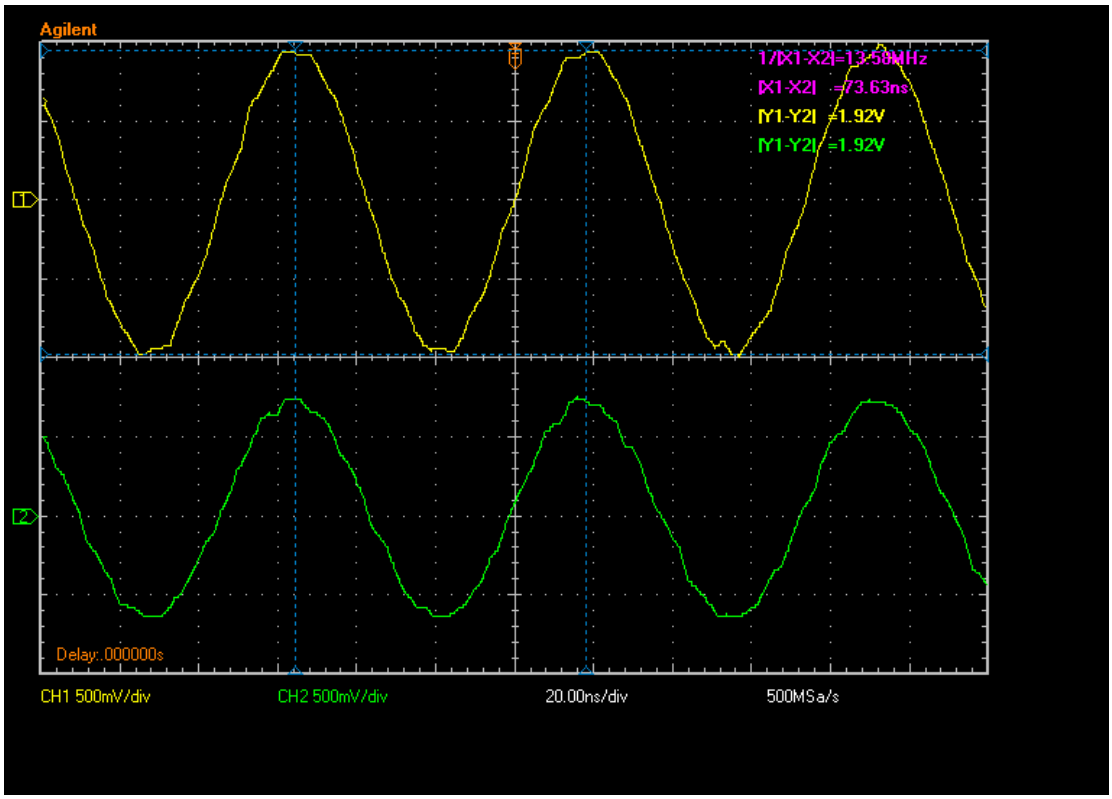

Fig. 15: Inductive Coupling Test Shows Battery Side (Yellow) and Sensor Side (Green) Signals

The next test checked that the rectifier portion of the circuit provided positive and negative DC voltage rails. This was done by keeping the same inductor orientation as in the previous test, and connecting the diode capacitor circuitry to the sensor side inductor. A 10 Vpp signal was fed through the downlink path, and an oscilloscope was used to read the two voltages. This created a 1.88V differential between the two rails. The voltage rails can be seen in Figure 16.

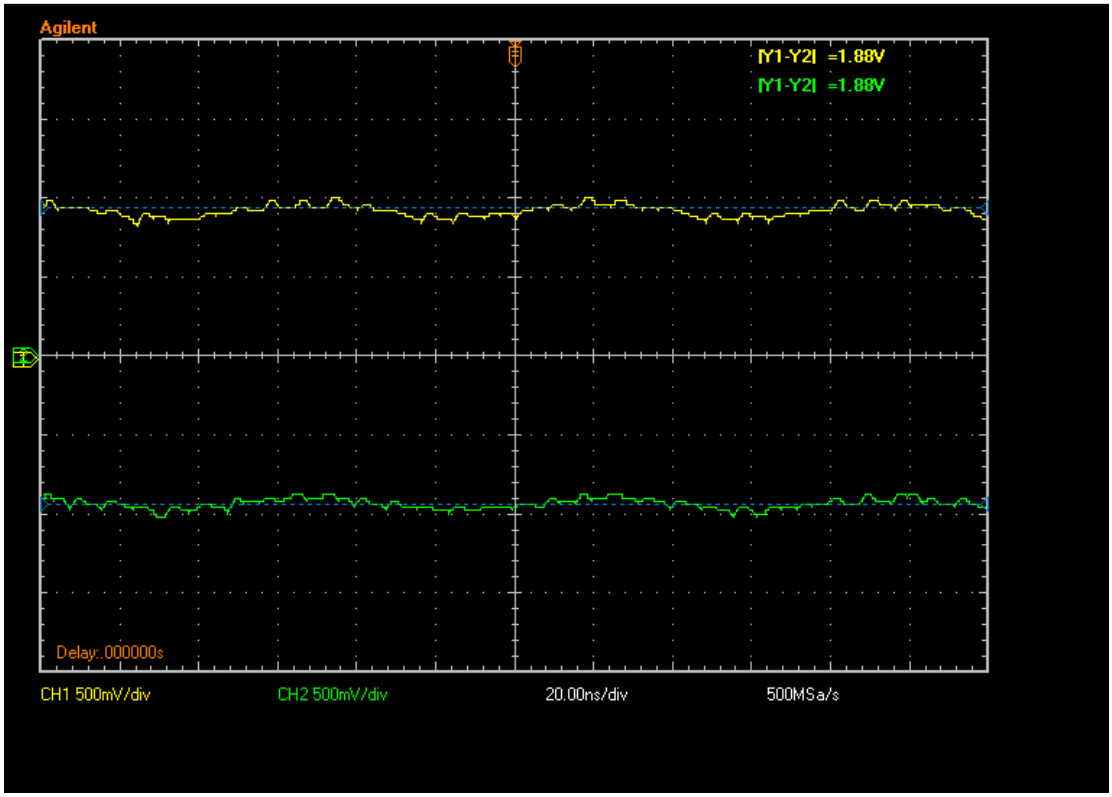

Fig. 16: DC Voltage Rails on Sensor Side

The final test dealt with feeding in the constant 13.56 MHz and a signal that acted as the digital sensor output by using function generators. The output was measured at the R1/L1 node shown in Figure 14. A 6 Vpp signal was fed in as the 13.56 MHz sinusoidal signal from the battery side, and a 3.5 Vpp square wave at 100 kHz was sent in as the digital sensor output. The results are shown in Figure 17.

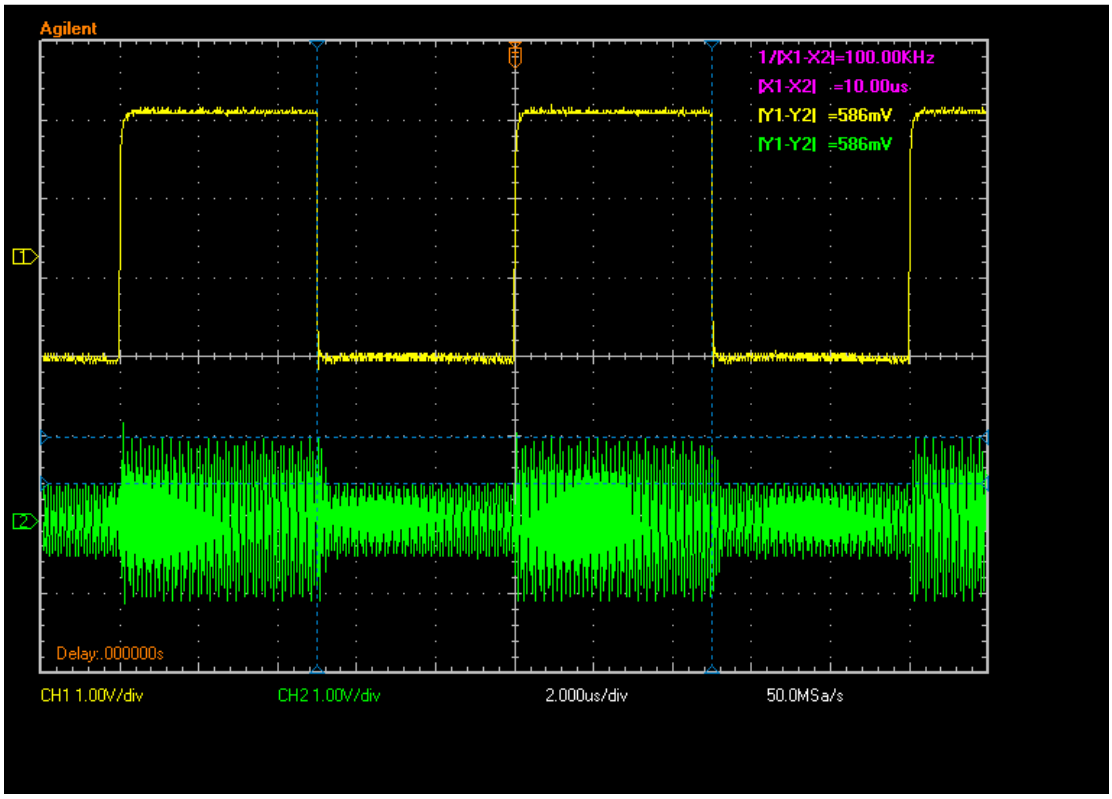

Fig. 17: Digital Sensor Output (Yellow) and Wirelessly Transmitted Data at R1/L1 Node (Green)

Figure 17 shows that the circuit is able to be wirelessly supplied with power via the downlink path, and simultaneously transmit digital data back via the uplink path. After testing this circuit, it is clear that it has the potential to one day replace the wired connection in modern neurological sensors and eliminate the need for a permanent hole to be left in the patient's skull.

VII. CONCLUSIONS AND RECOMMENDATIONS

This project analyzed chaotic signaling behavior associated with epileptiform activity, discussed modern medical devices used to detect and eliminate this activity, and presented an improvement to these devices. Many processes in nature have chaotic characteristics, and understanding the behavior behind these processes has many benefits. Understanding the chaotic behavior of neurons led to the creation of detection systems that can actively prevent seizures in many people suffering from epilepsy. There are still many advances to be made in this area. Leaving a permanent hole in patient's skull opens the patient up to increased risk of infection, less overall protection for the brain, and discomfort from the wiring. This project presented a solution to this issue. However, there are many areas to expand on this project that could benefit this technology. Moving into a higher frequency range would reduce the size of the near-field coupling structure, making it easier to implant. Also, integrating the entire sensor and DSP core together with more effective tuning for the system, or introducing a ferrite core into the inductors for better energy transfer would make the ECoG more accurate. Additional biological testing is essential, and more applicable to a smaller design. This includes finding an optimal frequency range for living bone, and measuring how much radiation the

brain absorbs when implementing a wireless system. However, this project acts as a proof of concept that a wireless system can be implemented.

VIII. BIBLIOGRAPHY

1. M. Dhamala, V. Jirsa, and M. Ding, Transitions to Synchrony in Coupled Burting Neurons, Vol. 92, No. 2, 2004
2. F. Sun, M. Morrell, and R. Wharen, Jr., Responsive CorticalStimulation for the Treatment of Epilepsy, Neurotherapeutics: The Journal of the American Society for Experimental NeuroTherapeutics, Vol. 5, No. 1, 2008
3. Kobylarz, Erik J., Nicholas D. Schiff, Theodore H. Schwartz, and Douglas R. Labar. *EXTERNAL RESPONSIVE NEUROSTIMULATION SYSTEM EFFECTS ON POWER AND COHERENCE SPECTRA OF INTRACRANIAL ELECTROENCEPHALOGRAPHY*. New York: Weill Medical College of Cornell University. PDF.
4. *Ncpn573989.fig3*. Digital image. *Medscape Today*. Nature Publishing Group, 2008. Web. 7 Dec. 2010. <http://www.medscape.com/viewarticle/573989_4>.
5. S. Strogatz, Nonlinear Dynamics and Chaos, p. 33-34, 1994

APPENDICES

A. Schematic

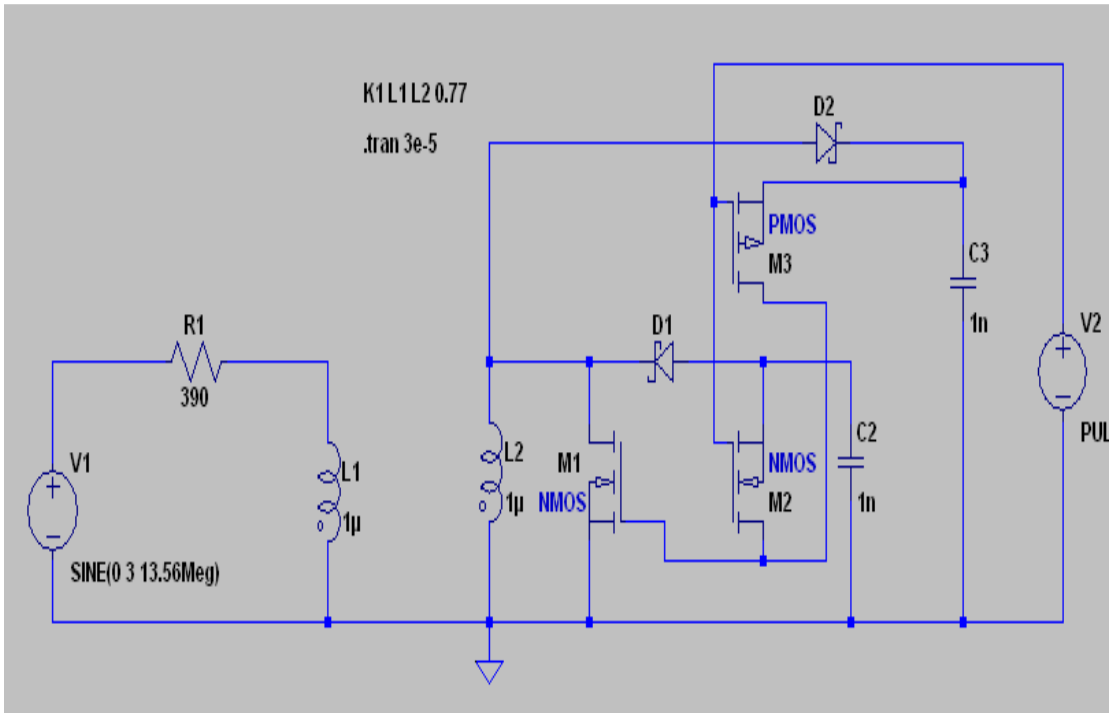

Fig. 18: Circuit Schematic

B. Parts List and Cost

Part	Unit Price ($)	Number	Total Price ($)
390 Ohm Resistor	0.10	1	0.10
1 nF Capacitor	0.10	2	0.20
5082-2835 Schottky Diode	0.08	2	0.16
CD4007UBE IC	0.25	1	0.25
Roll of Copper Tape	9.37	1	9.37

Table 1: Parts List and Cost

C. Time Allocation

Task	Estimated Time (Hours)	Actual Time (Hours)
Research	30	50
Coding	40	50
Design	30	40
Construction/Troubleshooting	10	20
Testing	10	10
Report	30	50
Total	150	220

Table 2: Time Allocation

D. Runge-Kutta Approximation

```
function [xnow,t]=RK4_wade(I);

% Original Author: Dr. Nilgun Sungar
% Code Adapted By: Wade Barnes

% this program solves a  3rd order system (3 coupled first order
differential equations)
% where the time series of the three variables are stored in the
array xn
% the differential equation xdot=f(x,y,z) isevaluated by the
function
% called xdot.

%clear all
%tic
h=0.005;     %this is  time increment
to=0;     %starting time
tout=3000;    %ending time
N=(tout)/h;   %number of time steps
t=linspace(to,tout,N);

% xo stored as column vector- why are these values chosen as initial
% conditions? semi-random initial condition?
xo=[-1.5*(1+0.1*randn); 0;3.2*(1+0.02*randn)]; %initialvalues

    x=xo;  % x is the array that holds the current values of the
three variables

% the following values stored as '0' column vectors
k1x=zeros(3,1);
```

```
k2x=zeros(3,1);
k3x=zeros(3,1);
k4x=zeros(3,1);
xn1=zeros(3,1);
xn2=zeros(3,1);
xn3=zeros(3,1);

% Is wp the frequency of oscillation for the external current?
wp=0;   %this is a parameter that is passed on to the function call
xdot
xn=zeros(3,N);
xn(:,1)=x;
for i=1:N-1
k1x=h*xdot_wade(i*h,x,wp,I);
xn1=x+k1x/2;
k2x=h*xdot_wade((i+1/2)*h,xn1,wp,I);
xn2=x+k2x/2;
k3x=h*xdot_wade((i+1/2)*h,xn2,wp,I);
xn3=x+k3x;
k4x=h*xdot_wade((i+1)*h,xn3,wp,I);
xn(:,i+1)=x+k1x/6+k2x/3+k3x/3+k4x/6;
x=xn(:,i+1);

end

xnow=xn(1,:);

figure(1)
subplot(3,1,1)
plot(t, xn(1,:));
grid on
xlabel('Time')
ylabel('x')
title(['External Current =  ' num2str(I)])

subplot(3,1,2)
plot(t, xn(2,:));
grid on
xlabel('Time')
ylabel('y')

subplot(3,1,3)
plot(t, xn(3,:));
grid on
xlabel('Time')
ylabel('z')
```

```
figure(2)
plot3(xn(1,:),xn(2,:),xn(3,:))
grid on
xlabel('x')
ylabel('y')
zlabel('z')
title(['External Current = ' num2str(I)])

figure(3)
plot(xn(1,:),xn(3,:))
grid on

toc
```

E. HR Neurons

```
function dy=xdot(t,y,wp,I)

% Original Author: Dr. Nilgun Sungar
% Code Adapted By: Wade Barnes

% y(1) is the membrane potential
% y(2) is associated with the fast current (Na+ or K+)
% y(3) is associated with the slow current (Ca2+)

a=1.0;
b=3.0;
c=1.0;
d=5.0;
r=0.006;
s=4.0;
xo=-1.6;

% stores dy as column vector
dy=[y(2)-a*y(1)^3+b*y(1)^2-y(3)+I*(1+0.1*sin(wp*t));c-d*y(1)^2-
y(2);r*(s*(y(1)-xo)-y(3))];
return
```

F. Bifurcation Map Generator

```
function spike_burst

% Author: Wade Barnes
```

```
I=linspace(1.5,4,400);
for m=1:length(I)
    i=0;
    [xnow,t]=RK4_wade(I(m));
    [spike,pos]=localmax(xnow,0.5);
    for n=1:length(spike)
        if spike(n)>0 && t(n)>(30*I(m))
            i=i+1;
            time(i)=t(n);
        end
    end
    for j=1:(i-1)
        if time(j+1)-time(j)>4
            per(j)=time(j+1)-time(j);
        end
    end
    for i=1:length(per)
        plot(I(m),per(i),'.','MarkerSize',1)
        xlabel('External Current')
        ylabel('Time Between Consecutive Spikes')
        hold on
    end
    clear per
end
```

G. Population Coupling

```
clear all

% Original Author: Dr. Nilgun Sungar
% Code Adapted By: Wade Barnes

h=0.05;  % delta-t  time step size
to=0;
tout=3000; % final time
N=(tout)/h; %number of time steps
t=linspace(to,tout,N);
I=3.2;

n=5;        %number of coupled systems
wp=0  %ignore this
coup=.9   %coupling strength
%initialize all in the array randomly
for i=1:n
xo(:,i)=[-1.5*(1+0.2*randn); 0;3.2*(1+0.2*randn)]
end
```

```
   x=xo; %set the value at t=0 to initialized arrays

k1x=zeros(3,n);
k2x=zeros(3,n);
k3x=zeros(3,n);
k4x=zeros(3,n);
xn1=zeros(3,n);
xn2=zeros(3,n);
xn3=zeros(3,n);


xn=zeros(3,n,N);
xn(:,:,1)=x;
for i=1:N-1   %for each timestep
    for j=1:n   %for each element in the chain
        if j==1   %for the very first one
            if i==1
k1x=h*xdot(i*h,x(:,j),wp);
xn1=x(:,j)+k1x/2;
k2x=h*xdot((i+1/2)*h,xn1,wp);
xn2=x(:,j)+k2x/2;
k3x=h*xdot((i+1/2)*h,xn2,wp);
xn3=x(:,j)+k3x;
k4x=h*xdot((i+1)*h,xn3,wp);
xn(:,j,i+1)=x(:,j)+k1x/6+k2x/3+k3x/3+k4x/6;
x(:,j)=xn(:,j,i+1);
            else
              per=coup*(x(1,n)+x(1,j+1)-2*x(1,j));  % coupling term
which couples to nearest neighboours
              k1x=h*xdotch(i*h,x(:,j),per);
              xn1=x(:,j)+k1x/2;
              k2x=h*xdotch((i+1/2)*h,xn1,per);
              xn2=x(:,j)+k2x/2;
              k3x=h*xdotch((i+1/2)*h,xn2,per);
              xn3=x(:,j)+k3x;
              k4x=h*xdotch((i+1)*h,xn3,wp);
              xn(:,j,i+1)=x(:,j)+k1x/6+k2x/3+k3x/3+k4x/6;
              x(:,j)=xn(:,j,i+1);
            end

elseif j<n   % for all the others except the last
    per=coup*(x(1,j-1)+x(1,j+1)-2*x(1,j));  % coupling term which
couples to nearest neighboours
    k1x=h*xdotch(i*h,x(:,j),per);
xn1=x(:,j)+k1x/2;
k2x=h*xdotch((i+1/2)*h,xn1,per);
xn2=x(:,j)+k2x/2;
```

```
k3x=h*xdotch((i+1/2)*h,xn2,per);
xn3=x(:,j)+k3x;
k4x=h*xdotch((i+1)*h,xn3,wp);
xn(:,j,i+1)=x(:,j)+k1x/6+k2x/3+k3x/3+k4x/6;
x(:,j)=xn(:,j,i+1);
        else    %this is for the last one which is coupled back to
the first one as well

         per=coup*(x(1,j-1)+x(1,1)-2*x(1,j));

    k1x=h*xdotch(i*h,x(:,j),per);
xn1=x(:,j)+k1x/2;
k2x=h*xdotch((i+1/2)*h,xn1,per);
xn2=x(:,j)+k2x/2;
k3x=h*xdotch((i+1/2)*h,xn2,per);
xn3=x(:,j)+k3x;
k4x=h*xdotch((i+1)*h,xn3,per);
xn(:,j,i+1)=x(:,j)+k1x/6+k2x/3+k3x/3+k4x/6;
x(:,j)=xn(:,j,i+1);
end
end
end

figure(1)
for ii=1:n
    a(1,:)=xn(1,ii,:);
    if ii==1
        plot(t,a,'b')
        hold on
        grid on
        axis([0 tout -2 2])
    elseif ii==2
        plot(t,a,'g')
        hold on
        grid on
        axis([0 tout -2 2])
    elseif ii==3
        plot(t,a,'r')
        hold on
        grid on
        axis([0 tout -2 2])
    elseif ii==4
        plot(t,a,'y')
        hold on
        grid on
        axis([0 tout -2 2])
    elseif ii==5
        plot(t,a,'k')
```

```
        hold on
        grid on
        axis([0 tout -2 2])
    end
end
xlabel('Time')
ylabel('x_n')
legend('x_1','x_2','x_3','x_4','x_5')
title(['External Current =  ' num2str(I) ' & Coupling Strength = '
num2str(coup) ])
```

H. Picture of Prototype

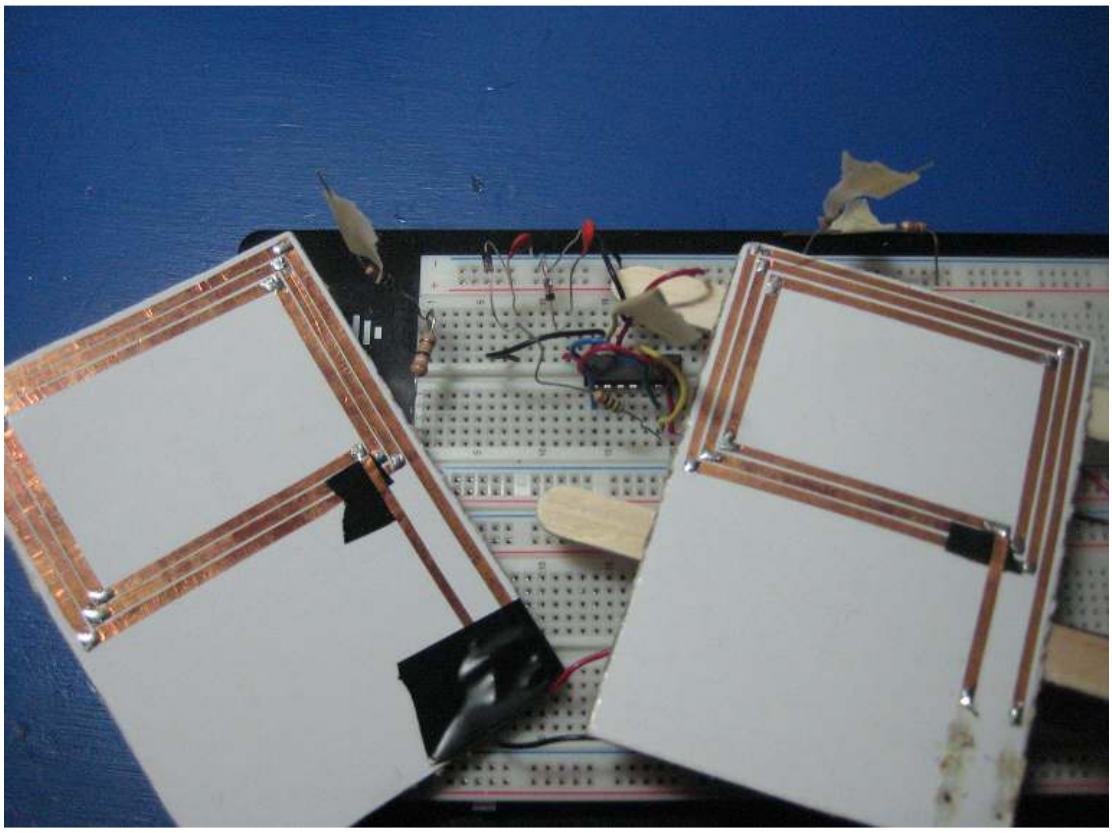

Fig. 19: Picture of Prototype